Selective laser melting of Inconel 601 alloy using nanosecond fibre laser

Raid Mohammed Hadi[1], Ziad Aeyad Taha[2]

[1, 2] Institute of Laser for Postgraduate Studies, University of Baghdad, Iraq

ABSTRACT

The paper describes the impact of selective laser melting factors including using a nanosecond fibre laser, including laser powers, scanning speed, and thickness of layer, on the relative density and micro hardness Vickers of IN 601 samples was studied. Selective laser melting (SLM) is a commonly used powder bed fusion metal additive manufacturing (AM). Recent advances in additive manufacturing have attracted significant industrial interest, especially for producing metallic parts. Scanning electron microscopy (SEM), EDX and other techniques were utilized for studying the effect of speed of scanning and power of laser on densification behaviour, microstructural evolution and micro hardness of Inconel v alloy that was processed by SLM. With a VED of 3200 J/mm³, a scan speed of 250 mm/s with a 80 W, micro cracks of about 79-93 µm and voids of about (4.5 µm – 5.7) µm in diameter were realised. Moreover, the best hardness of 394 HV was attained with 80 W laser power. However, increasing the energy to more than the required values increased the porosity and decreased hardness. Using microsecond laser in SLM leads to the achievement of full density (almost 99.5%), whereas using nanosecond laser allows the achievement of less density (75-95%), which will be very useful for functions that require a porous structure and less weight, such as those in the aerospace applications, automotive industry and so on.

Keywords: Nickel-Based Super alloys, Additive Manufacturing, Selective Laser Melting (SLM). Volumetric energy density.

Corresponding Author:

Raid Mohammed Hadi
Institute of Laser for Postgraduate Studies, University of Baghdad
Email: raed.mohammed1001a@ilps.oubaghdad.edu.iq

1. Introduction

Laser is widely used in many fields in the industry including welding, drilling, cleaning, ablation, etc. [1-3]. The new field for lasers in industrial is additive manufacturing these have a promising share in the present time. Inconel alloy is one of the most significant super alloys and is widely used in the petroleum and gas, marines nuclear and industries of jet engineering [4]. Inconel is a nickel-based superalloy that is widely used to make components for the aerospace, automotive and nuclear sectors because of its strong strength and resistance to creep. It also has good fabricability because of the low aluminium and titanium contents. The alloy could be perfect for selective laser melting, which may be used to create complicated components with high strength requirements [5]. Additionally, Inconel 601 (a high-performance alloy) generates a highly adhesive oxide scale under rigorous thermal cycling conditions, which helps prevent Spalling [6]. IN601 Alloys used in Chemical processing, pollution control, aerospace and power generation all benefit from lower Ni (61%) concentration with aluminium and silicon additives for increased oxidation and nitriding resistance [7]. The manufacturing industry has seen a huge breakthrough with additive manufacturing (AM). AM techniques build parts by depositing material layer by layer. Making AM a viable option for the complex-shaped parts for aircraft, vehicle, and biomedical implant usage [8, 9]. AM allows the development of highly complex geometries in metals, ceramics, composites and polymers that would be impossible to fabricate using a traditional method [10]. Owing to its capacity to handle a wide range of materials, the most popular AM method is the one that uses laser-based powder bed fusion (LPBF), selective technology of laser melting (SLM), for the creation of metallic components

with complicated geometries and outstanding characteristics [11]. SLM is an effective method used in additive manufacturing. In the manufacturing of mechanical parts, it can compete with existing technologies [12]. We could change standard SLM process variables, including laser powers, hatch spacing and scanning speeds, and layer thickness to improve the process [13].

Yasa et al. (2011) used different process parameters in laser re-melting, which showed the potential of this approach for improving the density and surfaces quality of SLM parts [14]. T.B. Sercombe et al. (2016) conducted a thorough analysis with the goal of establishing the impact of the Al-12Si powder surfaces chemistry on the components of Al-12Si porosity manufactured using SLM [15]. Tanja Trosch et al. (2016) explored the optimisation of SLM production of the characteristics that were superior to forged and cast material at room temperature. SLM-produced components displayed characteristics comparable with forged materials at increased temperatures due to a significant amount of intragranular delta phase [16]. Aqeel Ahmed et al. (2016) mentioned some research that compared porosity growth with heat input using the energy density idea [17]. Ali Gökhan Demir et al. (2017) investigated the viability of using an industrial SLM system to produce stent shapes. SLM was used as a replacement for the traditional manufacturing cycle. The evaluation was carried out with a pulsed wave, power-modulated fibre laser on an industrial SLM equipment designed primarily for medium-sized components [18]. Based on previously published research, Umberto Scipioni Bertoli et al. (2017) established a range of (VED) values that should result in the deposition of completely thick sections. The melting energy requirements for the alloys under study were compared with VED values used by other authors [19]. Zena J Wally et al. (2018) utilised the SLM procedure to create a variety of titanium micro-lattice structures using Ti-6Al-V [20]. Ahmed H et al. (2018) conducted a complete experimental investigation for evaluating the outcome of SLM process parameters on the quality of the manufactured Al alloys [21]. Jan Plat et al. (2020) explained that the so-called volumetric energy density (VED) can be calculated by using hatch distance and scan speed and by plugging in the laser powder, as well as by using layer thickness; such calculations would allow the SLM process to be regulated [10]. In the research of Davoud Jafaria et al. (2020), instead of utilising a traditional pressurised mould and heat source, they used SLM to create a sintered-like porous structure [22]. Alessia Teresa Silvertri et al. (2020) discussed the impact of the construction direction on the mechanical properties of the specimens; researchers tested AlSi10Mg specimens created with various SLM equipment [23]. Kaiwen Wei et al. (2020) studied titanium-based dual-alloy materials by using SLM to control the material performance of; specific technical concepts for the integrated fabrication of metallic structural components made of various titanium alloys were provided. [24]. Tian Xia et al. (2021) studied the solution and found that aging of the microstructure of the SLM-treated GTD222 was regulated through heat treatment [25]. Porosity is crucial in increasing fluid and heat transmission through porous structures. [24]. The degree of porosity in parts is a prominent topic in the AM industry. Considering that the pores enable greater Osseo integration with biological tissue, a degree of porosity, particularly surface-breaking porosity, is occasionally desired and can be designed into specific bio-medical implants [26]. Porous structures are used in a variety of applications, such as thermal energy storage systems, heat pipes, air conditioning systems, electronics cooling, gas turbines, fuel cells and chemical reactors [24].

In previous literature, a continuous laser and a microsecond laser were used to produce very high density for manufactured parts by selective laser melting, while in this study, a nanosecond fibre laser was used to produce a lower density and thus a lighter weight, which is suitable for many industrial applications including aerospace and automotive, as well as medical applications.

2. Materials and methods

The commercial Inconel 601 alloy powders with particle sizes ranging from 70 to 85 µm were used in the experiment with random shape. This research focused on Inconel 601 powder. The powder was placed in a furnace at 150 °C before the manufacturing process to eliminate moisture and reduce the temperature gradient during the building. All samples were fabricated by using the locally designed SLM apparatus, which employs an RFL-P100Q fibre laser with a wavelength of 1064 nm and a maximum power of 100 W measured in a pulse

mode of 81 nanosecond pulse duration. The powder morphology is shown in Fig. 1, which depicts that the alloy powder in general has sphericity and random shape. To observe the proportions of the elements contained in the alloy, we examined the energy dispersive X-ray spectrometry (EDX) to the alloy, as displayed in Fig. 2. The chemical composition of Inconel 601 alloy is illustrated in Table1. The locally designed SLM prototype system is shown in Fig. 3. This investigation was carried out with the goal of determining optimal parameters for experiment samples with moderate porosity. Cubic samples 5×5×5 mm^3 were made for this purpose on AISI 304 stainless steel building platforms. To prevent oxidation during the construction of IN601 cubic pieces, inert gas argon was used throughout the fabrication process, and a prototype system was locally designed. In the as-built state, samples that were constructed with a wide variety of energy inputs were evaluated. A set of variable parameters was created to determine the optimal parameter for manufacturing the sample. The best hatch distance was determined by adjusting power, speed and frequency. The best scan speed was determined by adjusting power, hatch distance and spot size. Fixing the speed and hatch spacing yielded the ideal spot size. In the meantime, the best power was chosen after fixing the scan speed, spot size and scan spacing, as presented in Table 2. Finally, the best VED was chosen after stabilising power and changing the speed. The energy density was computed by equation 1, as follows:

$$VED = \frac{p}{vhd} \text{ J/mm}^3 \text{ ----- (1)}$$

where VED is the volumetric powder bed density of energy (J/mm^3), P is the laser power (W), v refers to the laser scan speeds (mm/s), h the hatch distances (mm) and d is the thickness of the powder bed layer (mm) [27].

Table 1. Chemical composition Inconel 601alloy (Wt. %)

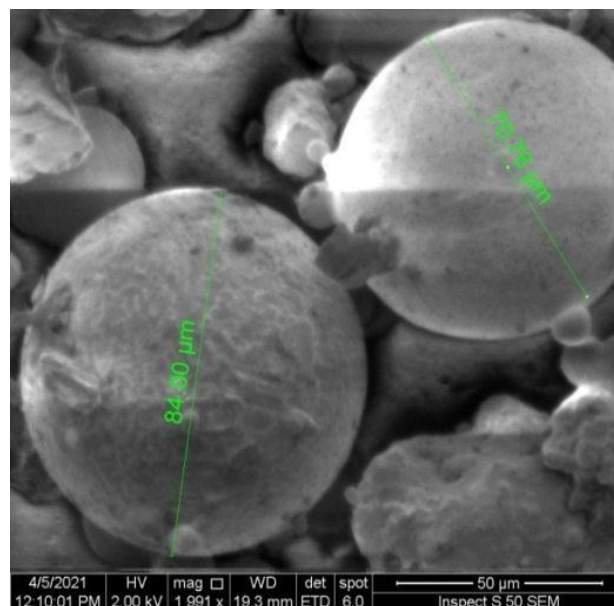| Elements	wt.%
Ni	Bal
Cr	23
Al	1.2
C	0.1
Mn	1
Cu	0.5
Si	1
S	--
Fe	15

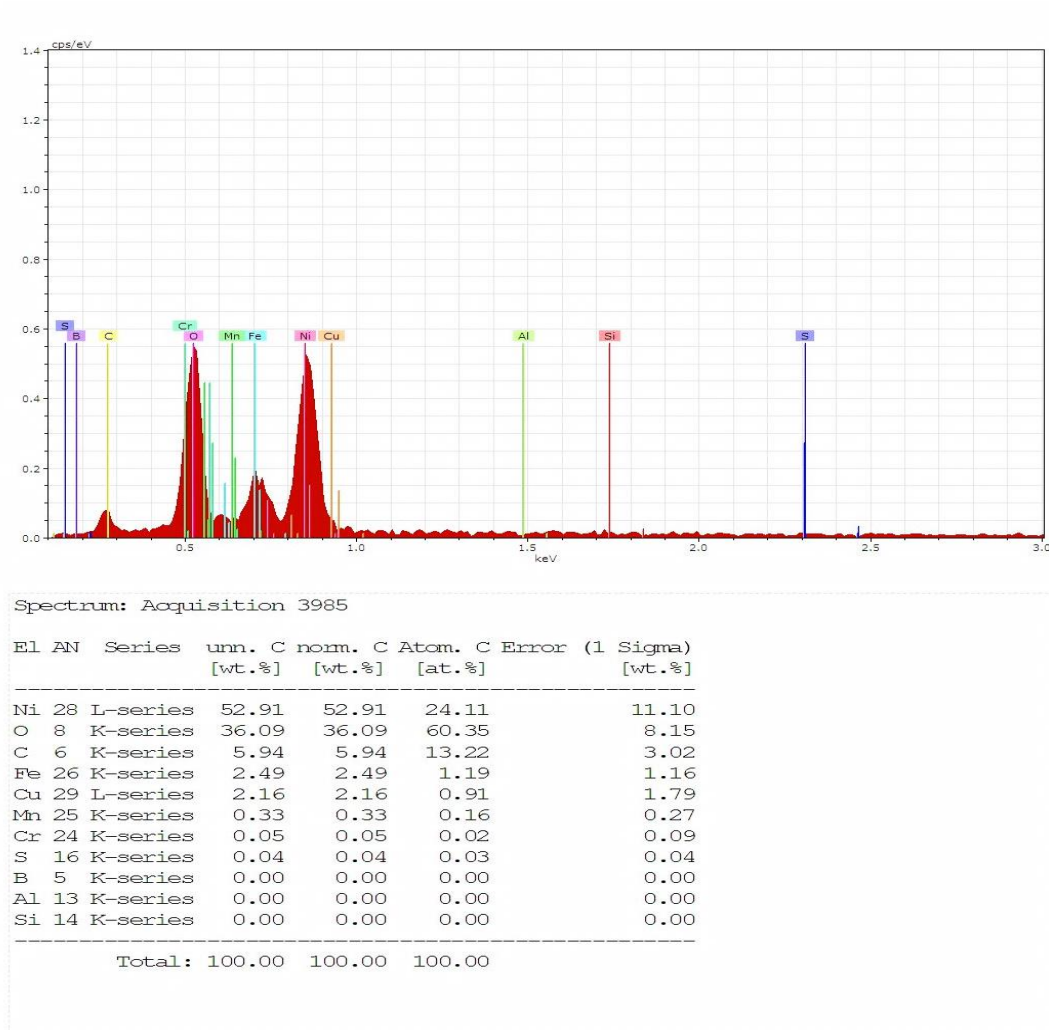Figure 1. SEM for powder Inconel 601 super alloy with random shape

Figure 2. EDX for powder Inconel super alloy

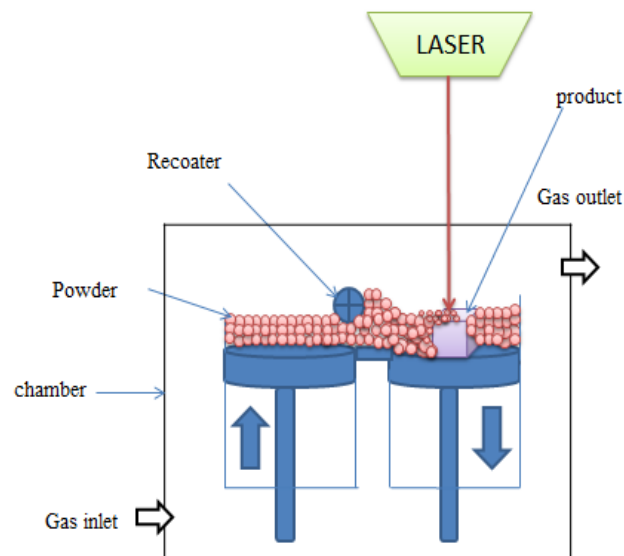
Figure 3. Schematic representation of (SLM) process prototype system locally designed

3. Results and discussion

It is difficult to prevent process-induced defects, such as pores caused by SLM process, non-optimal process factors, powder contaminations and local voids, that occur next to the layer deposition process. For example, cooling rate in the SLM preparation would result in higher remaining stresses, thereby causing warpage, breaking and base plate division. In this experiment, the input energy density effect on the porosity of the cubes was determined. A low level of energy density at (2000-2200 J/mm^3) provided a higher level of porosity and achieved the maximum level (35%) at the lowest energy density (2000 J/mm^3) due to the un-dissolved and partially dissolved powder particles. This situation arises due to the high velocity of 400 mm/s, which leads to insufficient melting. The laser paths are not wide enough to interfere with each other, and the particles are trapped between the paths. In Fig. 4, noticed that increasing the volumetric density by 2600 J/mm^3 reduces the porosity significantly. At 3200 J/mm^3 and at a speed of 250 mm/sec with the same capacity, the lowest porosity was found to achieve 5% minimum. When the volumetric density reached the level of 5000 J/mm^3 and higher, a sufficient amount of interference occurred in width and depth, which reduced the chance of leaving un-molten particles and thus increased the density of the produced part. This increased the porosity due to the low velocity (100-150 mm/sec), lead more heat being accumulated process by initialization vaporization that creates pores deeply, thereby producing a keyhole effect during operation. The pollutants evaporated because the high energy and low speed. The gas evaporated and left behind pores.

The scanning electron microscopy results in Fig. 5 reveal a sample with a volumetric density of 2000 J/mm due to the high speed, and the laser power was 80 watts. The particles caught between the laser paths were displayed. At the value of 3200 J/mm^3, the velocity was 250 mm/s, and laser power was 80 W, as shown in Fig. 6. Still, VED did not provide a complete picture for predicting melt pool behaviour or component density. Even if different melting parameters equated to the same VED, the result of these processes can be different. However, using different volumetric energy densities to measure densities of as-printed samples might provide a foundation for determining the SLM parameters required to melt a specific metal. In our work, the pulse duration was in nanoseconds (81ns). The value of VED differed from the VED values for microseconds and cannot be compared with other research papers. Fig. 7 shows that the best hardness was with at a laser of 80 watts. The laser power changed from an increment interval of 10 watts with the change of hardness. 394 HV was found to be the best with the stability of other parameters. Fig. 8 shows the relationship between hardness and scanning speed at a fixed laser power of 80 watts. Herein, the effect of the scanning speed was very important for the hardness. At a low speed, the hardness was low due to complete melting. High laser power leads to residual heat in the material, thereby decreasing in the cooling rate after the hardness was obtained. At high speed with the same power, incomplete melting of the material was observed, and thus, the hardness was also less. This result was due to the fact that the particles were not completely cohesive. The SEM image of Fig 9 shows the sample with a scanning speed of 350 mm/sec and a laser power of 80 W. Some particles did not completely dissolve for the above mentioned reason. The two types of pores created in Fig. 10 can be classified as keyhole and metallurgical pores. The latter are spherically formed and modest in size, while keyhole holes are irregularly shaped and huge in size (greater than 100μm) (less than 100μm). At slow scanning rates, trapped gases within the melt pool generate metallurgical holes. The keyhole instability, which can be linked to rapid metal solidification without complete filling of holes with molten metal, caused the keyhole pores. Figure 11 depicts the variations in the microstructure of different SLM-fabricated samples under various process settings. Based on microstructure and density, the green lines divide the changes into three sections, namely, near-total melting, partial melting and un-melted. The near-complete melting region's volumetric energy density was adequate to melt IN601 powder, but it was not high enough to create the key-hole effect. In the partially melted and un-melted areas. In Fig 12 shows the SEM image of the best-produced sample at 300x and 1300x magnification. It clearly shows the limited resulted porosity and micro-cracks due to the melt chosen work parameters.

Table 2. The most successful sample out of the whole group.

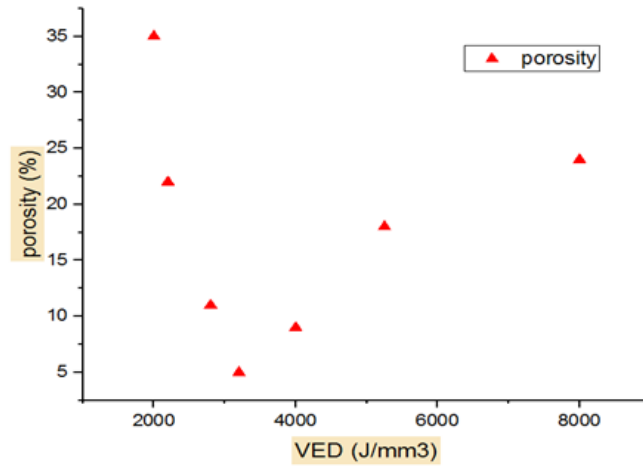|	
Laser powers (W)	80
Spot sizes (µm)	75
Frequencies (kHz)	40
Scan speeds (mm/s)	250
Layer thickness (mm)	0.1
Hatch spacing (mm)	0.001

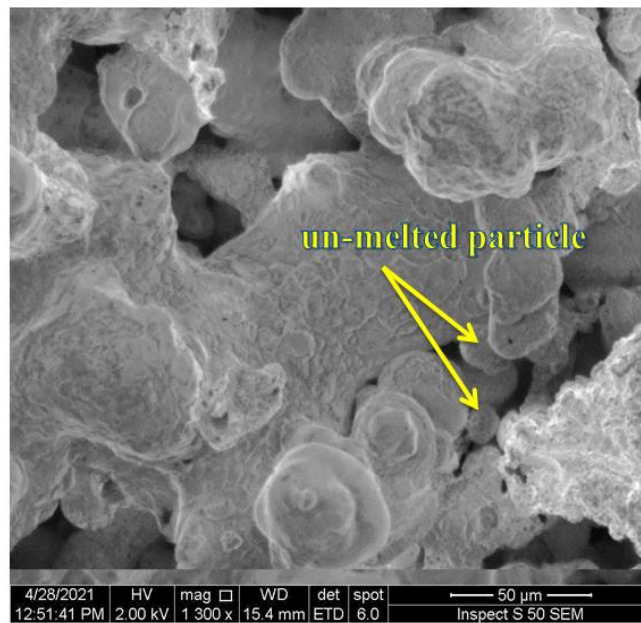Figure 4. VED of samples produced with deferent porosity

Figure 5. SEM showing porosity. Parameter: 80W-400mm/s, E. 2000J/mm^3
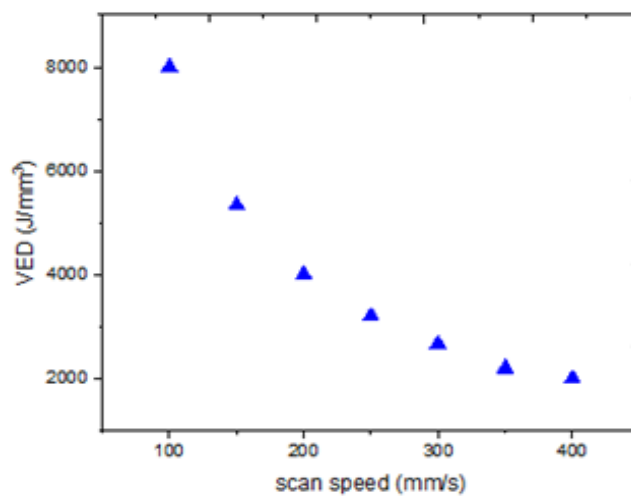

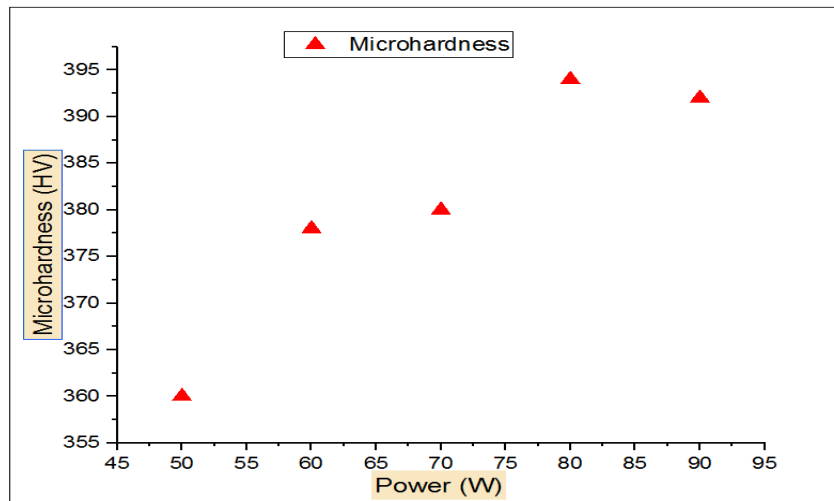Figure 6. VED of samples produced with different scan speed

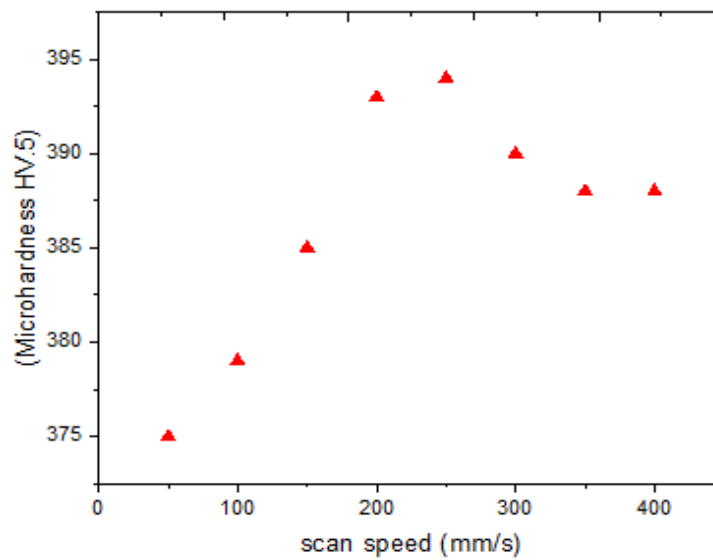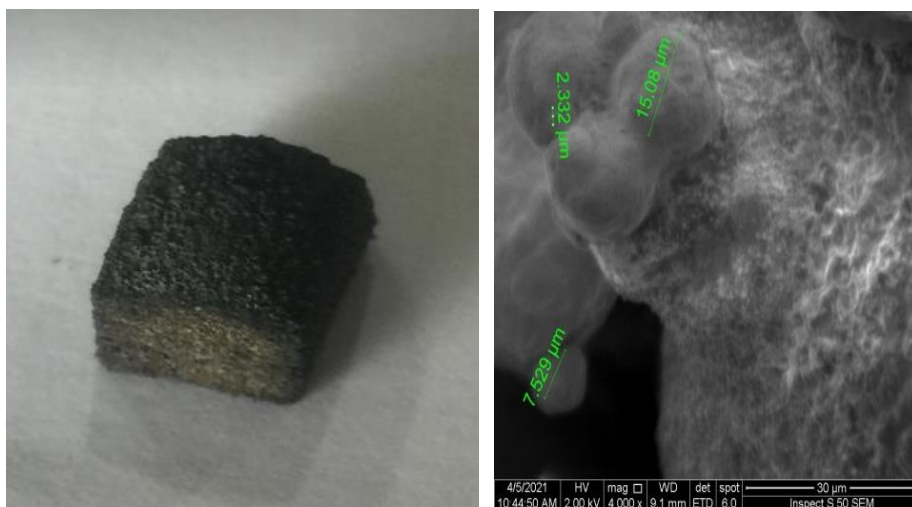Figure 7. Micro hardness HV of SLM samples fabricated by deferent LP

Figure 8. Micro hardness HV of SLM samples fabricated by deferent scan speed

| (a) | (b) |

Figure 9. (a) Sample image of Inconel 601 for scan speed 350 mm/sec, laser power 80 W, (b) SEM image of Inconel 601 sample with partial melting
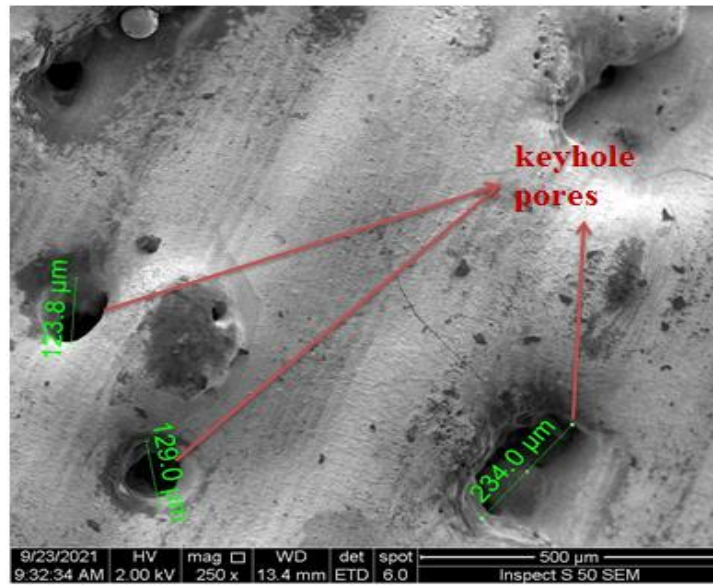
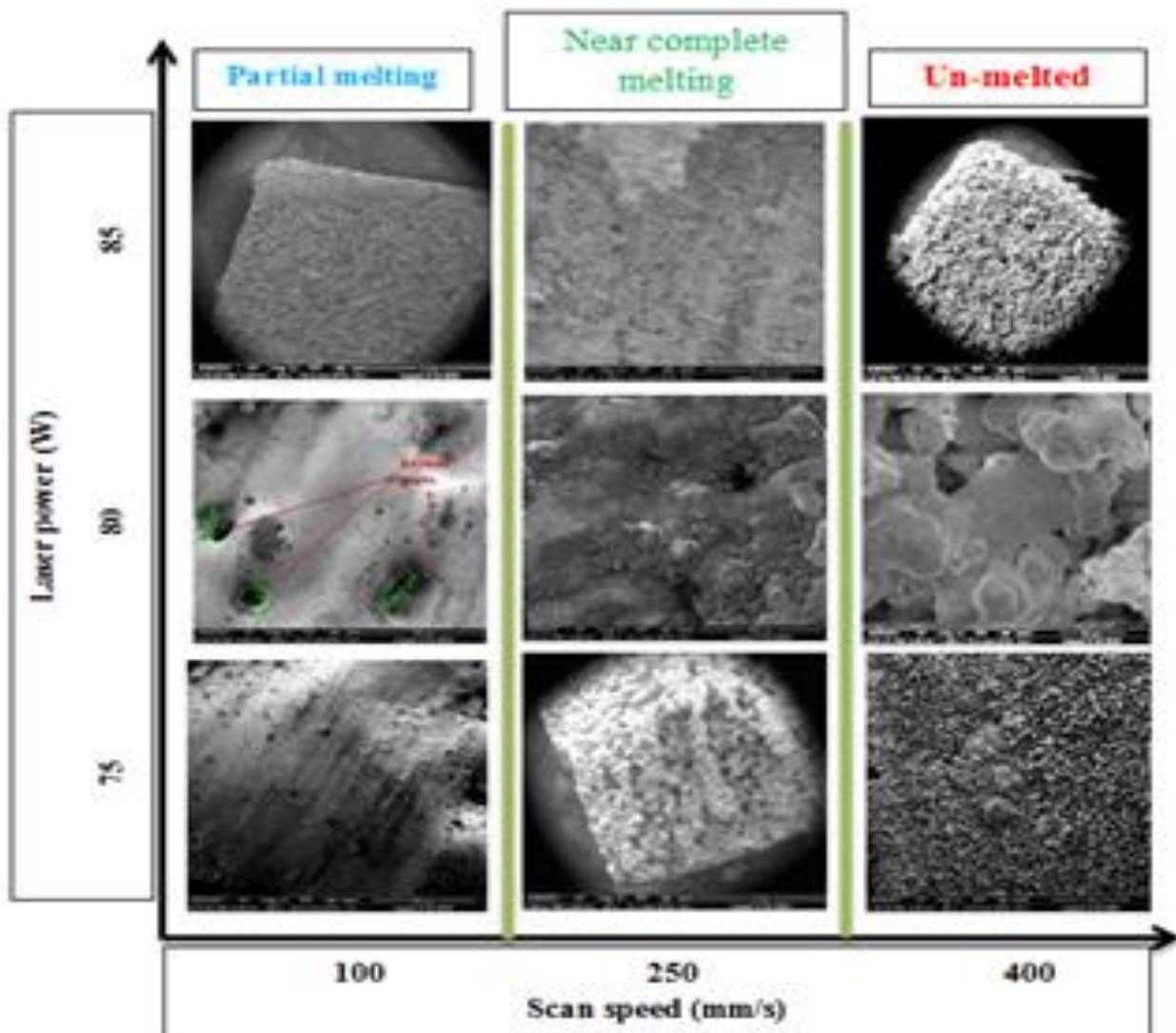Figure 10. SEM image of Inconel 601 sample with keyhole pores

Figure 11. SEM for microstructural. The near-complete melting, partial melting, and unmelted regions are divided by the green lines
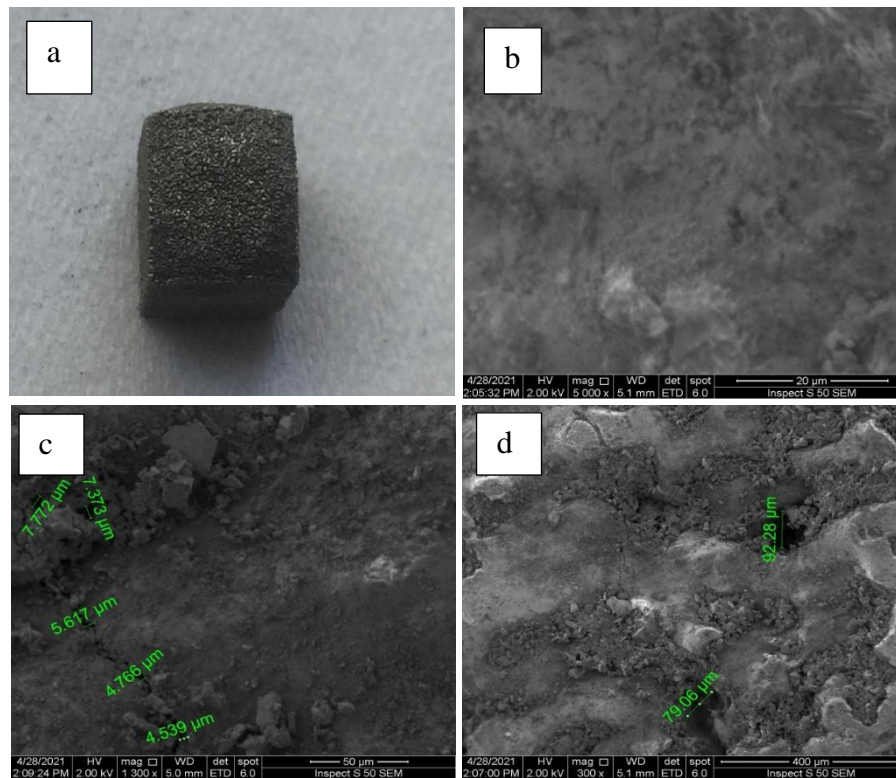
Figure 12. (a) Sample image of Inconel 601 for scan speed 250 mm/sec, 80 W, (b) SEM image showing near melting, (c) showing micro crack, (d) Showing limited porosity

4. Conclusion

One of the advantages of SLM is the design flexibility it affords, thereby allowing researchers to create regular porous structures for industrial and therapeutic applications. Porous metals have piqued researchers' curiosity for years, because they avoid stress-shielding effects by having reduced stiffness while still offering adequate mechanical strength. In this study, a nanosecond fibre laser was used to demonstrate the porous structures of IN601 alloys using SLM technology. The experiment showed that the use of high-intensity laser pulses to melt the selective layer of IN601 can have a positive effect on the melt flow, densification and porosity of the molten powder layers. This effect depended on process variables, such as scanning speed and laser power. Considering the large grain sizes of Inconel 601 in the (70-85) μm range, the super alloy elements revealed a quasi-porous character using a high-frequency nanosecond fibre laser. Cracks were found across a wide range of process parameters. Some process parameters also showed pores in the samples, whereas others revealed massive metallic pores due to the increased energy density.

The proportion of cracks and porosity was higher at lower scanning rates, according to the microstructure investigation, because the formation of metallic pores at these speeds was produced by gases inside the melt pools or formed by the powder in the consolidations. This experiment also showed that when the energy density ratio was increased, the fine hardness was decreased due to the occurrence of material brittleness as a result of higher temperatures in the product material.

Declaration of competing interest

Reference

[1] Z. A. Taha," Hole drilling of high-density polyethylene using Nd: YAG pulsed laser", *Iraqi Journal of Laser*, vol. 18, no. 2, pp.41- 46,2019.

[2] H. A. Jasim, G. A. Demir, B. Previtali, and A. Z. Taha, " Process development and monitoring in stripping of   a highly transparent polymeric paint with ns-pulsed fiber laser," Optics & Laser Technology, vol. 93, pp. 60-66, 2017.

[3] A. F. Mutlak, M. Jaber, and H. Emad," Effect of Laser Pulse Energy on the Characteristics of Au Nanoparticles and Applications in medicine," *Iraqi Journal of Science*, PP. 2364-2369, 2017.

[4] Z. Baicheng, X. Mingzhen, *"*Pitting corrosion of slm Inconel 718 sample under surface and heat treatments," *Applied Surface Science,* vol (490), PP. 556-567, 2019.

[5] M.C. Karia, M.A. Popat, and K.B. Sangani," Selective laser melting of inconel super alloy-a review," *AIP Conference Proceedings*, vol. 1859, no.1, ID, 020013, 2017.

[6] C . Upadhyay, S. Datta, M. Masanta, and S. S. Mahapatra," An experimental investigation emphasizing surface characteristics of electro-discharge-machined Inconel 601," *Journal of the Brazilian Society of Mechanical Sciences and Engineering*," vol. 39. No. 8, pp. 3051-3066, 2017.

[7] E. Akca, and A. Gürsel," A review on superalloys and IN718 nickel-based inconel superalloy," *Periodicals of Engineering and Natural Sciences* (PEN), vol. 3, no 1, 2015.

[8] Li. Yuze, M. Založnik, J. Zollinger, L. Dembinski, and A. Mathieu," Effects of the powder, laser parameters and surface conditions on the molten pool formation in the selective laser melting of IN718," *Journal of Materials Processing Technology,* 289, 116930, 2021.

[9] B. Durakovic," Design for Additive Manufacturing: Benefits, Trends and Challenges," *Periodicals of Engineering and Natural Sciences***,** Vol. 6, No.2, pp. 179-191, 2018.

[10] J. Platl, H. Leitner, C. Turk, A. G. Demir, B. Previtali , and R. Schnitzer, 2021, Defects in a laser powder bed fused tool steel. *Advanced Engineering Materials*, vol. 23, no. 12, 2000833, 2021.

[11] O. O. Salman, C. Gammer, J. Eckert, M. Z. Salih, E. H. Abdulsalam, K. G. Prashanth, and S. Scudino," Selective laser melting of 316L stainless steel: Influence of TiB2 addition on microstructure and mechanical properties,"*Materials Today Communications*, 21, 100615, 2019.

[12] L. Caprio, L., A. G. Demir, and B. Previtali., 2018," Comparative study between CW and PW emissions in selective laser melting," *Journal of Laser Applications*, vol. 30, no.3 , 032305, 2018.

[13] C. Y., Yap, C. K., Chua, Z. L Dong, Z. H., D. Q. Liu, Zhang, L. E., Loh, and S. L Sing," Review of selective laser melting: Materials and applications. *Applied physics reviews,* vol.2, no 4, 041101, 2015.

[14] E. Yasa, and J. P. Kruth," Application of laser re-melting on selective laser melting parts," *Advances in Production engineering and Management*, vol. 6, no. 4, PP. 259-270, 2011.

[15] X.P. Li a, K.M. O'Donnell and T.B. Sercombe," Selective laser melting of Al-12Si alloy: Enhanced densification via powder drying," *Additive Manufacturing,* vol. 10, PP. 10-14, 2016.

[16] T. Trosch, J. Strößner, R. Völkl and U.Glatze," Microstructure and mechanical properties of selective laser melted Inconel 718 compared to forging and casting," *Materials letters*, vol. 164, PP. 428-431, 2016.

[17] A. Ahmed, M. S. Wahab, A. A. Raus , K. Kamarudin , Q. Bakhsh1 and D. Ali,", Effects of selective laser melting parameters on relative density of AlSi10Mg," *Int. J. Eng. Technol,* vol. 8,no. 6, PP. 2552-2557,2016.

[18] A. G. Demir, and B. Previtali," Additive manufacturing of cardiovascular CoCr stents by selective laser melting*," Materials & Design,* vol. 119, PP. 338-350,2017.

[19] U. S. Bertolia , A. J. Wolferb , M. J. Matthewsc , J. P. R. Delplanqueb , J. M. Schoenung, On the limitations of volumetric energy density as a design parameter for selective laser melting. *Materials & Design,* vol. 113, PP. 331-340, 2017.

[20] Z. J. Wally, A. M. Haque, A. Feteira, F. Claeyssens, R. Goodall, and G. C. Reilly," Selective laser melting processed Ti6Al4V lattices with graded porosities for dental applications," *Journal of the Mechanical Behavior of Biomedical Materials*, vol. 90, PP. 20-29, 2019.

[21] A. H. Maamoun, Y. F. Xue, M. A Elbestawi, and S. C. Veldhuis,"Effect of SLM Process Parameters on the Quality of Al Alloy Parts; Part I: Powder Characterization*, Density, Surface Roughness, and Dimensional Accuracy,*" 2018.

[22] D. Jafari, W. W. Wits, T. H. Vaneker, A. G. Demir,B. Previtali, B.J. Geurts, and I. Gibson," Pulsed mode selective laser melting of porous structures: Structural and thermophysical characterization," *Additive manufacturing,* vol. 35, 101263, 2020.

[23] A. T. Silvestri, A. Astarita, A. El Hassanin, A. Manzo, U. Iannuzzo, G. Iannuzzo, and A. Squillace, 2020, Assessment of the mechanical properties of AlSi10Mg parts produced through selective laser melting under different conditions. *Procedia Manufacturing,* vol 47, PP. 1058-1064, 2020.

[24] K. Wei, X. Li. F, Zeng, M. Liu, and J. Deng, *"*Microstructure and mechanical property of Ti-5Al-2.5 Sn/Ti-6Al-4V dissimilar titanium alloys integrally fabricated by selective laser melting," *Jom :the journal of the Minerals, Metals & Materials* Society ,vol. 72,no. 3, PP. 1031-1038,2020.

[25] T. Xia, R. Wang, Z. Bi, G. Zhu, Q. Tan, and J. Zhang," Effect of heat treatment on microstructure and mechanical properties of a selective laser melting processed ni-based superalloy GTD222," *Materials*, vol. 14, no. 13, 3668, 2021.

[26] J. A, Slotwinski, E. J, Garboczi," Porosity of additive manufacturing parts for process monitoring. In *AIP* conference proceedings American Institute of Physics, vol. 1581, No. 1, pp. 1197-1204, 2014.

[27] S. Bai, N. Perevoshchikova, Y. Sha, and X. Wu," The effects of selective laser melting process parameters on relative density of the AlSi10Mg parts and suitable procedures of the Archimedes method", Applied Sciences, vol. 9, no. 3, 583, 2019.